

Storminess-related rhythmic ridge patterns on the coasts of Estonia

Ülo Suursaar^a and Hannes Tõnisson^b

^a Estonian Marine Institute, University of Tartu, Mäealuse St. 14, 12618 Tallinn, Estonia; ulo.suursaar@ut.ee

^b Institute of Ecology at Tallinn University, Uus-Sadama 5-537, 10120 Tallinn, Estonia; annu@tlu.ee

Received 29 March 2017, accepted 14 September 2017, available online 10 November 2017

Abstract. Buried or elevated coastal ridges may serve as archives of past variations in sea level and climate conditions. Sometimes such ridges or coastal scarps appear in patterns, particularly on uplifting coasts with adequate sediment supply. Along the seacoasts of Estonia, where relative-to-geoid postglacial uplift can vary between 1.7 and 3.4 mm/yr, at least 27 areas with rhythmic geomorphic patterns have been identified from LiDAR images and elevation data. Such patterns were mainly found on faster emerging and well-exposed, tideless coasts. These are mostly located at heights between 1 and 21 m above sea level, the formation of which corresponds to a period of up to 7500 years. Up to approximately 150 individual ridges were counted on some cross-shore sections. Ten of these ridge patterns that formed less than 4500 years ago were chosen for detailed characterization and analysis in search of possible forcing mechanisms. Among these more closely studied cases, the mean ridge spacing varied between 19 and 28 m. Using land uplift rates from the late Holocene period, the timespans of the corresponding cross sections were calculated. The average temporal periodicity of the ridges was between 23 and 39 years with a gross mean value of 31 years. Considering the regular nature of the ridges, they mostly do not reflect single extreme events, but rather a decadal-scale periodicity in storminess in the region of the Baltic Sea. Although a contribution from some kind of self-organization process is possible, the rhythmicity in ancient coastal ridge patterns is likely linked to quasi-periodic 25–40-year variability, which can be traced to Estonian long-term sea level records and wave hindcasts, as well as in regional storminess data and the North Atlantic Oscillation index.

Key words: beach ridge systems, coastal scarps, sea level, storms, Holocene, climatic cycles, LiDAR.

INTRODUCTION

A beach ridge is a wave-swept or wave-deposited coastal geomorphic feature running parallel to a shoreline. It is composed of sorted sand or coarser sediment worked out from the sea bottom. Beach ridges are widespread worldwide and can be considered as common features on many types of coasts (Scheffers et al. 2012). Quite often, individual beach ridges gradually join together and form spits, or appear as extensive rhythmic patterns, visible from aerophotographs or large-scale topographic maps. Estonian seacoasts are rich in beach ridges and coastal spits. These are finger-like accumulative embankments diverging from the mainland and being built up of beach material as a result of longshore sediment transport. Fresh beach ridges and recurving spits have been extensively studied in Estonia over the last decades (e.g. Rivis 2004; Orviku et al. 2009), including the effect of storms and sea level variations on their gradual evolution and development (Suursaar et al. 2013; Tõnisson et al. 2013, 2014). Speaking of older shore formations, the features which correspond to the

Litorina Sea (i.e., 7500–4000 cal yr BP – calendar years before present) coastlines, can be frequently found at heights of 20–30 m in Estonia (Saarse et al. 2007) and some coastal marks from the Ancylus Lake (9500–8000 yr BP) can be found on the altitudes of up to 45 m (Kessel & Raukas 1967).

Although studies on coastlines from different Baltic Sea development stages have long traditions in Estonia (e.g. Orviku 1974; Raukas & Hyvärinen 1992), earlier investigations were not able to resolve microrelief over broad areas using high-accuracy altimetry data and therefore missed the patterns. Thus, apart from individual landforms, the mid- and late Holocene (0–8200 yr BP) coastal ridge systems have neither been catalogued nor thoroughly studied in Estonia before. Thanks to the introduction of new study methods, such as use of ground-penetrating radars (GPRs; Vilumaa et al. 2016, 2017) or LiDAR (Light Detection and Ranging; also: light and radar) surveys, it has become evident that in addition to contemporary beach ridges, a number of ancient, buried or elevated coastal ridge and scarp systems can be found in various regions, not far landwards from the sea (Fig. 1).

© 2017 Authors. This is an Open Access article distributed under the terms and conditions of the Creative Commons Attribution 4.0 International Licence (<http://creativecommons.org/licenses/by/4.0>).



Fig. 1. Map of Estonia with enumerated beach ridge systems (see Table 1) and tide gauge stations.

A number of studies on beach ridge systems exist worldwide (e.g. Taylor & Stone 1996; Nielsen et al. 2006; Hayes et al. 2010; Nott et al. 2015). However, there seems to be no commonly accepted or universal explanation for their development, as both morphological properties and forcing conditions vary widely. Nevertheless, some important fundamental facts have been established. Beach ridge systems as depositional geomorphic features occur only at specific suitable sections of the coast. A flat coastal topography with a sufficient sediment supply, dominating accumulation and sufficiently strong wave energy are usually needed to move a significant amount of material, against gravity, in order to build up ridges (Taylor & Stone 1996; Allard et al. 2008). Ridges built up from coarser material can gradually grow higher during successive storms, and, in contrast to sandy ridges, are not eroded by them. Medium- and low-category storms are considered more ‘constructive’ compared to strong-category cyclones, which tend to be more ‘destructive’ (Scheffers & Scheffers 2006). Beach ridges on sandy coasts are constructed more often during moderate wave conditions and severe storm conditions may initiate the erosion of the existing ridges (Furmańczyk et al. 2011).

Aeolian processes as well can easily reform such ridges (Anderson et al. 2014). It is often difficult to detect the main factor forming the sand-built rhythmic patterns: the wind or hydrodynamic agents (waves, sea level variations, currents) or a combination of both. Apparent

sea level lowering at a location is also an important factor for beach ridge development. The preservation of beach ridge systems is possible if new ridges are gradually elevated and placed out of reach of shore processes. Therefore, beach ridge sequences are often considered a source for reconstructing past environmental changes such as sea level variations, storm intensities or tsunamis (Buynevich et al. 2007; Tamura 2012; Nott 2004).

The key questions regarding the genesis of beach ridge systems are as follows. (1) What kind of processes dominate the morphodynamics of beach ridge systems: episodic, periodic or long-term processes? (2) If there is a periodicity present in beach ridge systems, what are the responsible forcing mechanisms? (3) Can the forming conditions of beach ridges be forecasted or extrapolated to the future. This article addresses these questions alongside presenting a regional overview and description of Estonian rhythmic beach ridge systems.

MATERIAL AND METHODS

LiDAR data and identification of rhythmic patterns

Although some areas with rhythmic coastal landscape patterns can also be detected from aerial photographs or in the field (Hara–Juminda region; Osmussaar Island; Fig. 2), their identification and characterization owes a great deal to LiDAR surveys, which, in Estonia, have



Fig. 2. An oblique (not to scale) aerial photograph of the SE tip of Osmussaar Island taken by the Estonian Land Board (*Maa-amet*) (No. 833944) on 21 April 2016. The length of the indicated transect No. 15 (including approximately 39 beach ridges) is 550 m and the age span is about 1070 years.

been carried out by the Estonian Land Board. Using an aircraft-borne aero-laser scanner Leica ALS50-II, a survey of the Estonian territory was first performed in 2008–2011, and again in 2012–2015. Since then, the elevation data have been made available on a web-based geoportal (geoportal.maaamet.ee/eng/) or through the Land Board.

Our methodology for studying the genesis of the beach ridge systems in Estonia is as follows. First, we viewed the elevation data on the geoportal to assess the past and present Estonian coastline (up to a height of approximately 25 m) in order to identify areas displaying the rhythmic patterns of interest. At least 27 such locations, mainly along the western and northern coasts of Hiiumaa Island and northern Estonian mainland (Fig. 1, Table 1), were identified. The actual number of areas with rhythmic patterns is even larger, but those that were too faint or too old or covered by peat or fragmental structures were not included in the study. (It is interesting to note that one rhythmic pattern may have been identified within the Tallinn city limits in the Pirita–Mähe–Kloostrimetsa region at an elevation between 16 and 23 m. The age (approximately 5000–8000 yr BP; see Fig. 3) of such features suggests that the patterns had been levelled and transformed as a result of natural processes and human intervention.)

Second, some of the beach ridge systems with more extensive and clearer patterns were selected for more detailed investigation. For those areas, we ordered raw LiDAR elevation data from the Estonian Land Board. Using ArcGIS software, digital elevation models in raster format were created from the LiDAR data. Angular shading (illumination with azimuth 315° and altitude 30°) was used in ArcGIS in order to develop more visually contrasting patterns on 2D images (Fig. 4). The coordinates of the LiDAR measurement points appear in raw elevation data only in the L-EST97 (LAMBERT-EST) system, with initial coordinates $x_0 = +6375\ 000\ \text{m}$ and $y_0 = +500\ 000\ \text{m}$, and the elevations in the BK77 system (using EST-GEOID 2011 model). For broader viewing options, the L-EST97 coordinates were converted into geographical coordinates (in decimal degree format), usable in the geoportal, GIS and other formats such as Google Maps.

Depending on the 2400 m aircraft flight level, the average density of the LiDAR points was 0.45 p/m² during the first Land Board surveys, the maximum distance between the dots was 2.6 m, the calculated precision of the height estimate was 0.07–0.12 m and the actual vertical precision was in the range of ±0.34 m according to the control measurements on the field (e.g. Gruno et al. 2013). However, the accuracy and those

Table 1. Overview of cross sections through some of the rhythmic beach ridge systems in Estonia (Fig. 1). Lat, latitude (N); Lon, longitude (E); Exp, shore exposition direction; Alt R, altitude range (m a.s.l.); L, total profile length (km); LU(G), land uplift rate relative to geoid (mm/yr) (Suursaar & Kall 2017). The locations for detailed description (Table 2) are shown in bold

No.	Location	Lat	Lon	Exp	Alt R	L	LU(G)
1	Tahkuna	59.08°	22.61°	NE	4.5–8.5	1.4	3.4
2	Lõimastu	59.08°	22.63°	N	4.5–8.0	0.7	3.4
3	Lehtma	59.07°	22.67°	NE	3.0–8.5	1.5	3.4
4	Suurjärv	59.04°	22.64°	NE	7.5–16.0	1.6	3.3
5	Tareste	59.01°	22.68°	NE	2.0–16.5	3.5	3.3
6	Kanapeeksi	59.00°	22.68°	NE	2.0–18.5	4.1	3.2
7	Mänspe	58.82°	22.51°	W	2.0–16.5	4.0	3.2
8	Õngu	58.85°	22.49°	SW	6.0–19.0	3.9	3.1
9	Mardihansu	58.88°	22.43°	SW	6.0–15.0	1.0	3.2
10	Kõpu	58.94°	22.08°	NW	12.5–16.0	0.7	3.4
11	Tagalaht	58.40°	22.10°	N	2.0–16.0	2.7	2.7
12	Pammana	58.61°	22.54°	NW	2.0–20.0	3.3	2.7
13	Hõbringi	59.15°	23.56°	W	3.0–16.0	3.0	3.0
14	Rannaküla	59.23°	23.65°	NW	2.0–5.5	0.9	3.1
15	Osmussaar	59.28°	23.42°	SE	0.8–4.0	0.5	3.2
16	Keibu	59.24°	23.78°	NW	4.0–17.5	3.4	3.1
17	Pedase	59.26°	23.92°	NE	5.5–16.0	1.7	2.9
18	Väike-Pakri	59.35°	23.95°	NW	4.0–12.0	1.3	3.1
19	Treppoja	59.36°	24.28°	SW	12.0–18.0	1.3	2.8
20	Jõesuu	59.49°	25.19°	NW	3.0–6.5	0.5	2.8
21	Pudisoo	59.53°	25.57°	W	2.0–13.0	1.3	2.7
22	Loksa	59.59°	25.72°	NW	4.5–9.0	1.0	2.7
23	Odakivi Bay	59.64°	25.70°	NW	1.0–14.0	0.8	2.8
24	Käsmu	59.57°	25.88°	NW	1.0–6.5	0.8	2.7
25	Altja	59.58°	26.13°	N	4.5–21.0	0.8	2.6
26	Letipea	59.53°	26.60°	NW	4.0–15.5	1.8	2.3
27	Narva-Jõesuu	59.44°	28.05°	NW	7.0–12.0	0.8	1.7

error margins regarding the vertical datum were not critical to this study, as we further studied relative height differences along transects.

Third, some cross-shoreline sections were drawn and ArcGIS trigonometric tools were used to assess the corresponding height profiles (Fig. 5). Depending on the areal density and precision of the LiDAR elevation readings, the calculations from the elevation model height profile data have a horizontal step of 0.5 m and vertical step of 0.01 m. We believe that this allows the detection of landscape features from a relative horizontal scale of approximately 1–2 m and a height scale of about 0.1–0.2 m.

Finally, the height differences between the starting and terminal points of the profiles were matched with land uplift rates in order to calculate the age differences over the individual profile sections and to calculate the spatial and temporal spacing of the subject ridges. This last step required us to estimate local (apparent) land uplift rates.

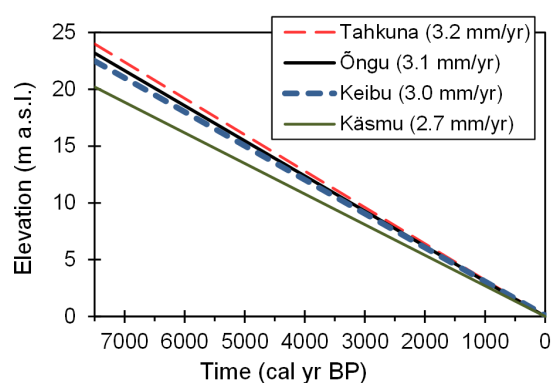


Fig. 3. Simplified apparent water level curves as a result of postglacial uplift and water volume change over the last 7500 years in the regions of the Tahkuna Peninsula and Õngu (according to Vassiljev et al. 2015), and Keibu Bay and Käsmu (according to Grudzinska et al. 2013). Over the last 100–150 years an accelerating modern-era global sea level rise has introduced a ~30 cm bend in the curve (which is barely visible). Also, according to e.g. Lambeck et al (2014), the eustatic sea level rise has not been linear over the late Holocene; the rise rate probably was approximately 0.2 mm/yr in 0–4200 cal yr BP, but slightly faster earlier.

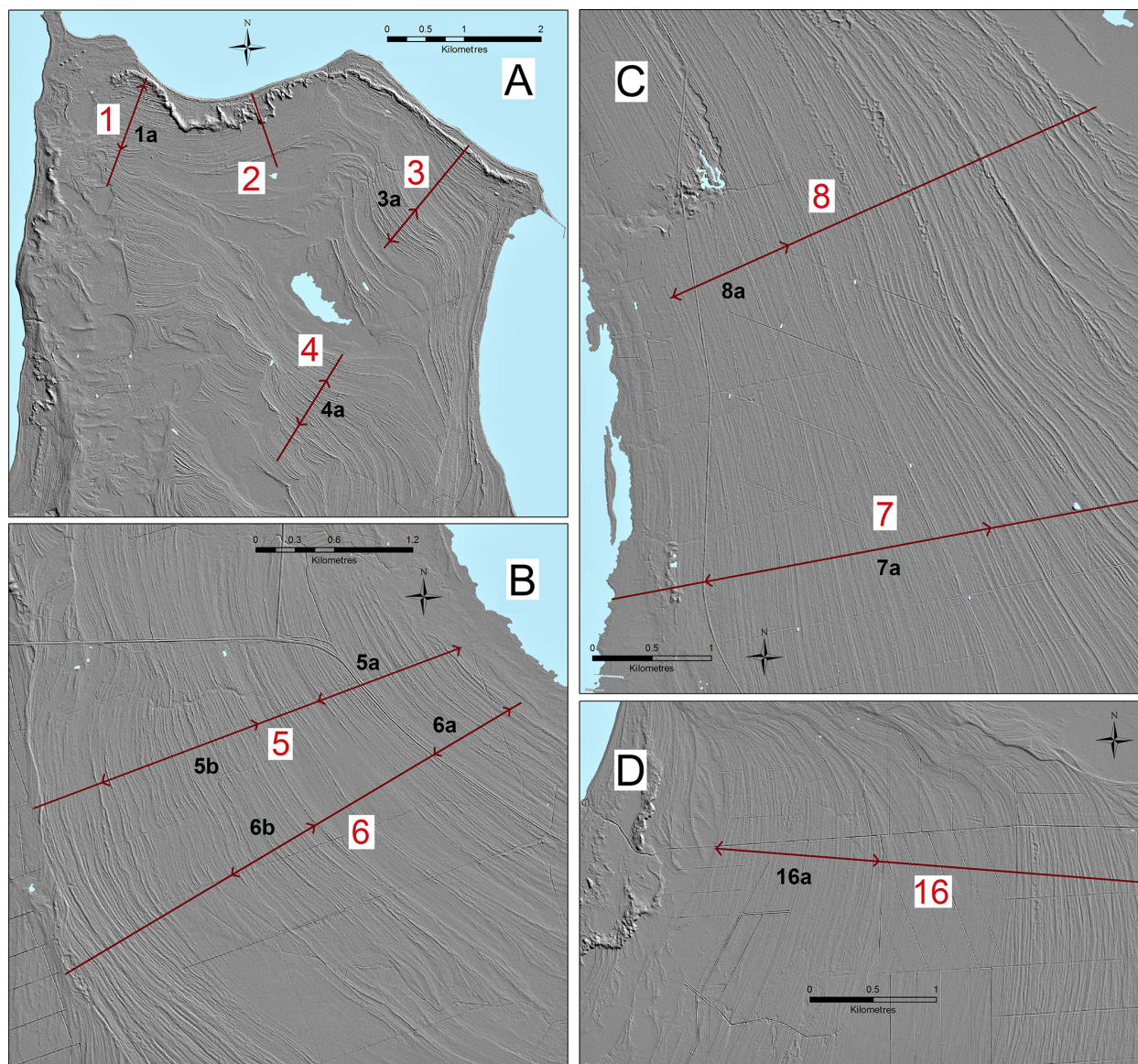


Fig. 4. Images created using LiDAR elevation data from Hiiumaa Island (A, B, C) and the Keibu region (D). See Fig. 1 for the locations of the enumerated full-length profiles and Table 1 for the coordinates and lengths. The direction of the profiles is away from the beach; specific profile sections are indicated (see also Table 2).

Relative sea level, land uplift and met-ocean forcing data

In response to the glacio-isostatic rebound of the entire Fennoscandian region, a relative sea level fall (or in other words, apparent land uplift) occurred during the mid- and late Holocene period in Estonia (e.g. Ekman 1996; Saarse et al. 2007). Finding exact rates for those changes, however, is not an easy task.

One idea was to use tidal gauge time series, which provide relative sea level data extending back for several

centuries in the Baltic Sea. In Estonia, the oldest sea level series began in 1840 (in Tallinn). Unfortunately, the trends calculated from such data are strongly influenced by contemporary global sea level rise (GSLR), and therefore cannot be used for most of the Holocene. Although it might seem fruitful to combine the local relative sea level trend rates with the commonly accepted GSLR rate, the result does not match with local apparent land uplift rates. One reason for that lies in the fact that local sea level rise may considerably deviate from the GSLR (which is a worldwide weighted average over a specific period

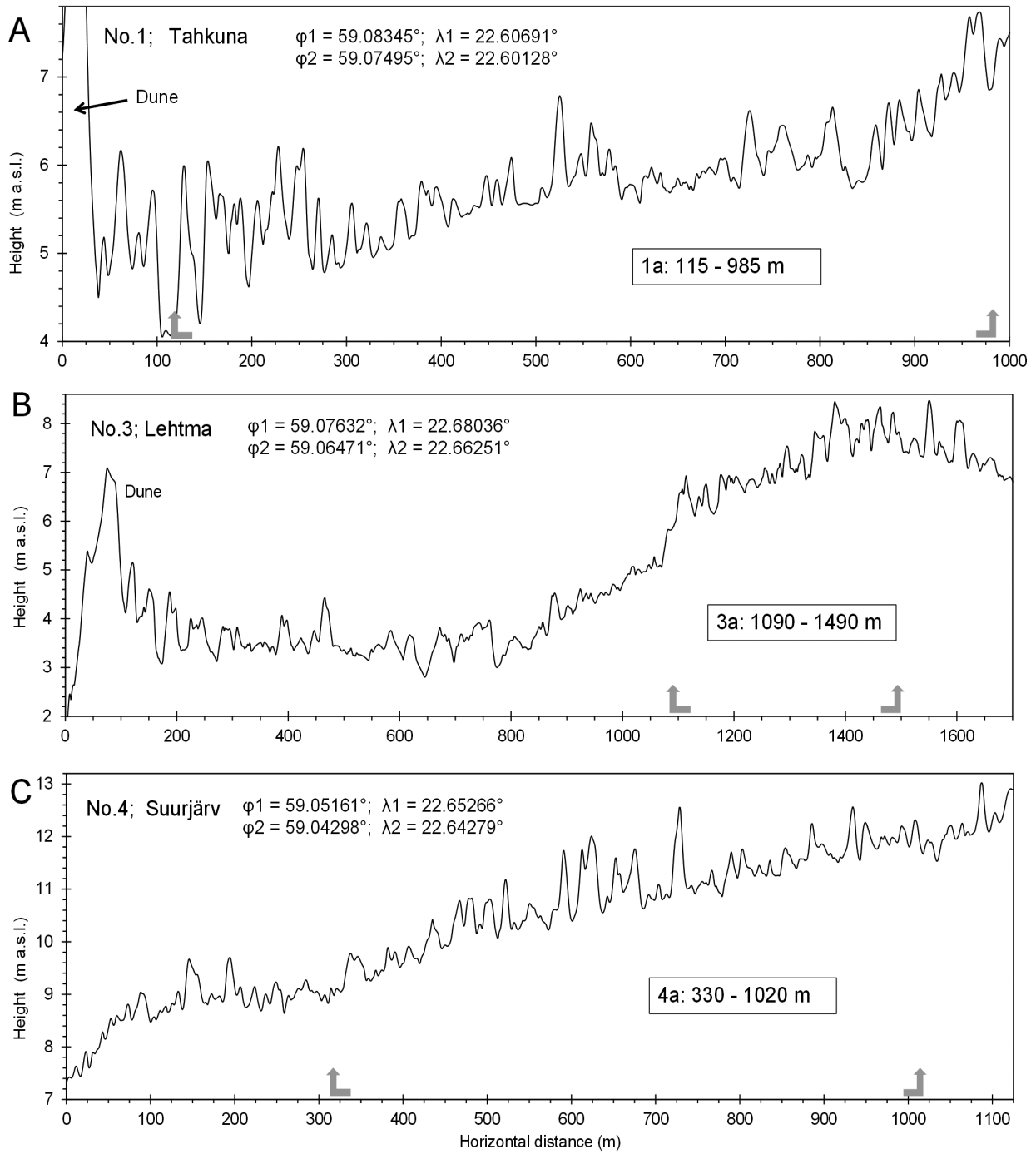


Fig. 5. Excerpts of height profiles (see also Tables 1, 2 and Figs 1, 4). Geographical latitudes (φ , N) and longitudes (λ , E) are given for initial (φ_1 , λ_1) and terminal (φ_2 , λ_2) points of the excerpted selections. The length spans used in the statistics (Table 2) are indicated with arrows and in the text boxes. (Continued on the next page.)

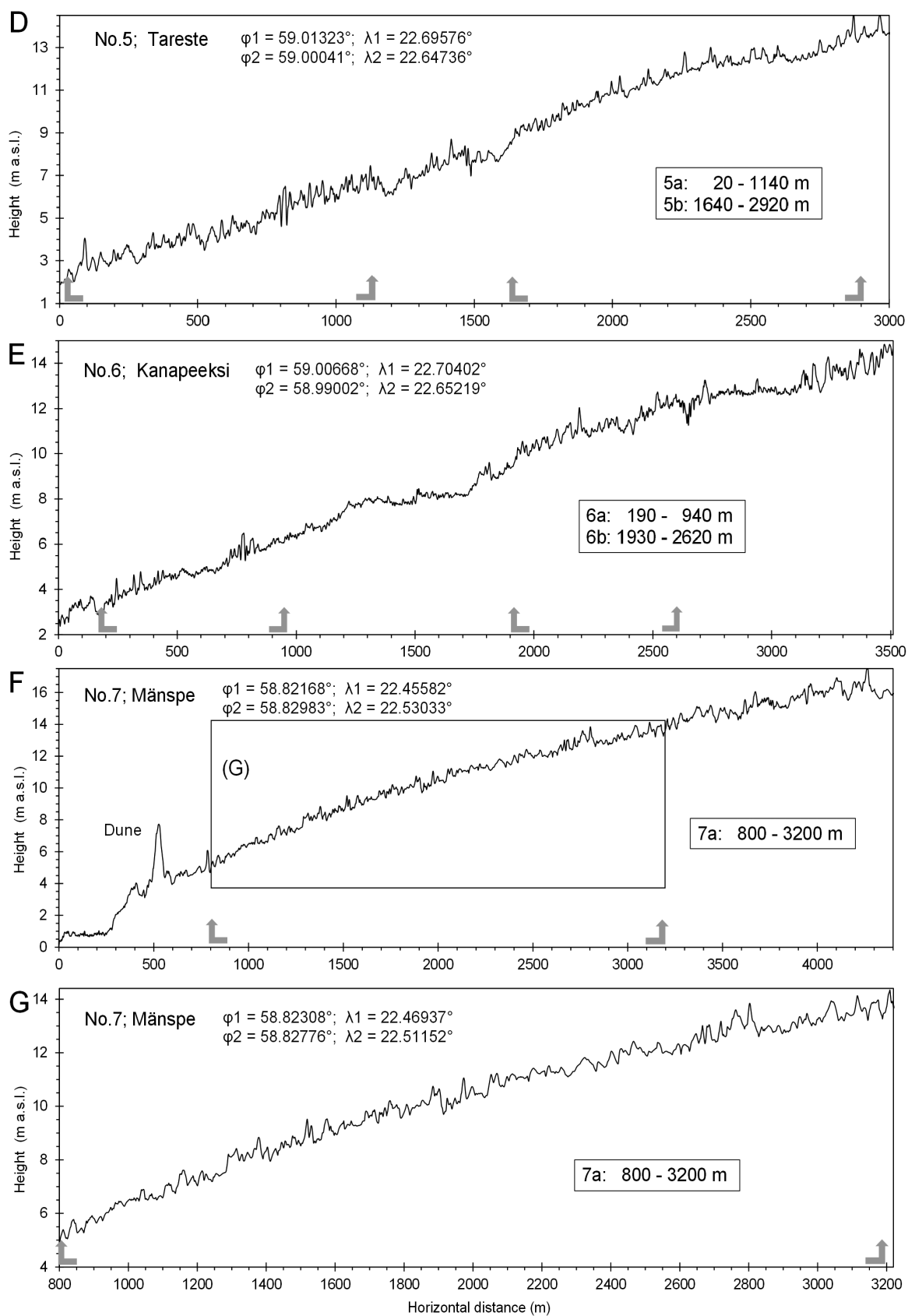


Fig. 5. Continued. (Continued on the next page.)

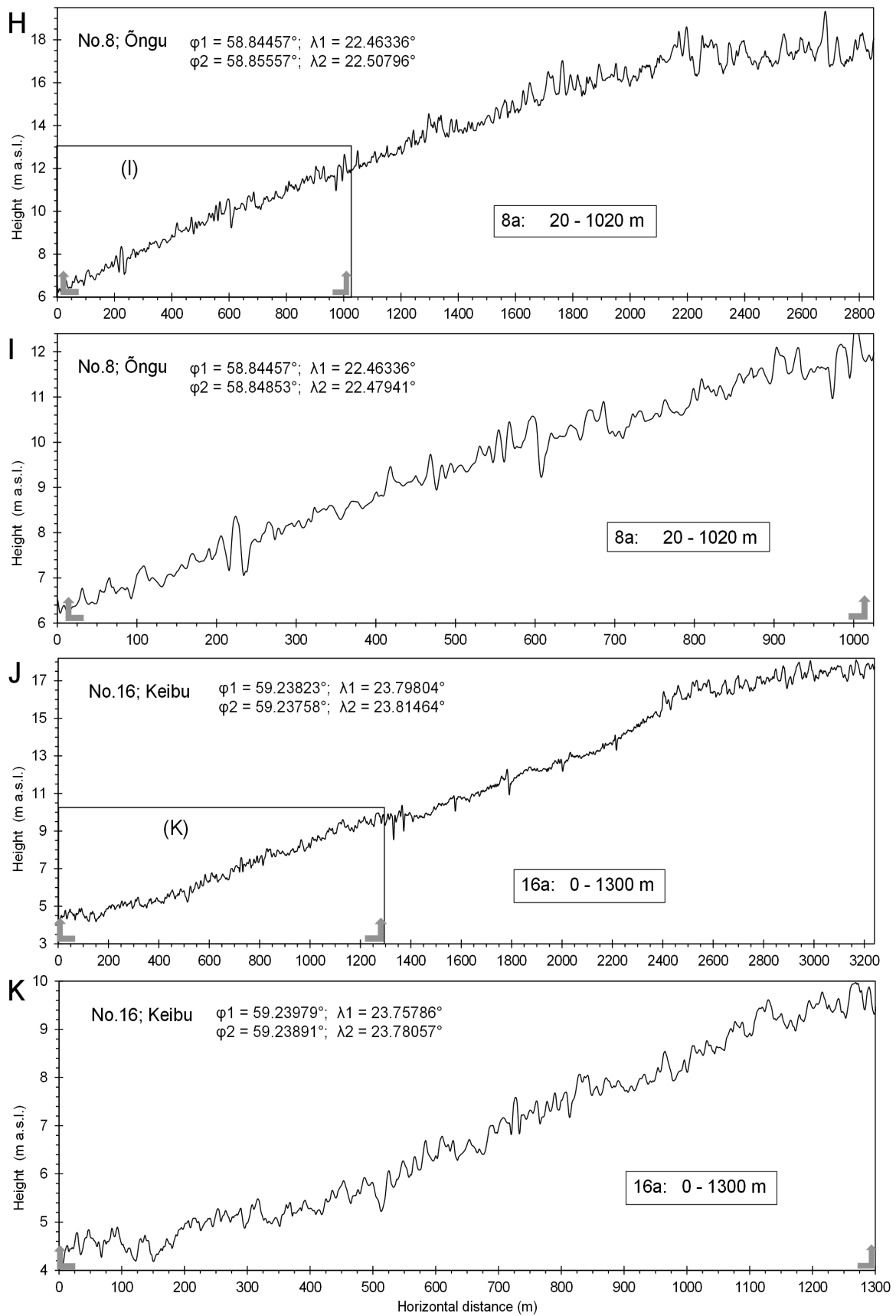


Fig. 5. Continued.

of time value; Church et al. 2013). For instance, using a trend analysis of Estonian tide gauge data and the most recent land uplift rates relative to geoid, Suursaar & Kall (2017) found that ‘local sea level rise’ was, depending on the tide gauge, about 0.5–1 mm/yr faster than the GSLR over the same period. The difference came primarily from large inter-annual sea level variability in the Baltic Sea in reaction to changing wind conditions (Suursaar & Kullas 2006; Johansson & Kahma 2016), which operate both on a local scale (e.g. as variations in the Baltic semi-permanent sea level tilt) and on a regional scale (e.g. Cronin et al. 2014). These variables have changed considerably over the last hundred years, which makes their inclusion in trend analyses or contemporary apparent uplift maps difficult.

Another idea was to use so-called apparent land uplift maps, which are based on repeated levellings and models of Scandinavian isostasy. Indeed, a series of gradually improving uplift maps have been available in the past (e.g. Vallner et al. 1988; Ekman 1996; Torim 2004; Kall et al. 2016). However, such maps are less reliable predictors of land uplift rates in the mid- and late Holocene period, as somehow they include a share from contemporary time-varying GSLR, and probably also the poorly resolved sea level difference between the Baltic Sea and the World Ocean. New Scandinavian uplift maps have recently been compiled (Vestøl et al. 2016), which do not depend on accelerating sea level rise and therefore are appropriate for this study. A fragment of the relative-to-geoid land uplift (LU(G)) model NKG2016LU_lev covering only Estonia was published by Suursaar & Kall (2017). According to Simpson et al. (2015), the relative-to-geoid model should be the appropriate one for sea level applications; the LU(G) values in Table 1 were taken from that map fragment.

It should be noted that the LU(G) values differ from the apparent uplift rates presented in fig. 4 of Kall et al. (2016) by about 0.5–1 mm/yr. On the other hand, the LU(G) values can be verified with the rates from relative sea level lowering curves (over the last 7500 years; Fig. 3). More specifically, based on various litho-, bio- and chronostratigraphical proxies, the mid- and late Holocene shoreline changes have been reconstructed and published for various locations of Estonia (Saarse et al. 2007; Grudzinska et al. 2013; Vassiljev et al. 2015; Muru et al. 2017; Fig. 3). The uplift rates vary along the Estonian coast and such curves are not available in many locations, but where they do exist, the differences from the LU(G) values in Table 1 are negligible (between 0 and 0.2 mm/yr).

Indeed, over a time span of the last few millennia (but excluding the last 100–150 years), the relative-to-

geoid uplift rate should be a good proxy for relative sea level lowering in the Baltic Sea. It has become widely accepted that the global sea level became nearly stable after final meltwater pulses from the last glaciation episode in the mid-Holocene (e.g. Scheffers et al. 2012; Vassiljev et al. 2015). Still, according to some latest estimates (e.g. Lambeck et al. 2010, 2014; Cronin et al. 2014), the eustatic sea level rise, though slow, was not linear within the last 7500 years either. It could have been about 0.2 mm/yr over the period from approximately 4200 to 150 yr BP. About 1880–1900, the industrial-era accelerating sea level rise began, which has elevated the global sea level by about 25–30 cm (Church et al. 2013). On the other hand, before ~4200 yr BP, the eustatic sea level rise was probably somewhat faster as well. According to Lambeck et al. (2014), ~3 m sea level rise occurred in the interval 6700–4200 yr BP; according to Lambeck et al. (2010), the sea level likely rose by ~2.5 m to near present levels from 7000 to 3000 yr BP. This non-linearity is not large, but still may introduce an up to 10% deviation from the LU(G) rates used by us. This was the main reason why we decided not to use older sections (~4500–7500 yr BP) of the LiDAR profiles and mostly focused on those between the ages of 1000 and 4000 years. Also, in order to minimize the possible effect from the above-discussed eustatic sea level component, we subtracted 0.2 mm/yr from the LU(G) values in order to obtain our ‘apparent uplift rates’ for the late Holocene (Table 2).

In order to interpret the cyclic geomorphic shore processes, we used sea level measurements taken by the Estonian Environmental Agency, which cover the period of 1840–2016. Annual relative sea level data from three tide gauges were used in this study: Ristna (N 58.92°, E 22.07°), Tallinn (N 59.46°, E 24.82°) and Narva-Jõesuu (N 59.46°, E 28.03°). The studied coastal landscapes are situated roughly between these tide gauges (Fig. 1). Although not quite suitable for estimating sea level lowering over a longer period of time, the sea level records can serve as a proxy for determining decadal variations in local storminess, because high average and maximum sea levels are associated with storms and stormy periods in Estonia (Jaagus & Suursaar 2013). Also, variations in the North Atlantic Oscillation (NAO) index were used for a similar, illustrative purpose. In particular, we used the December to March station-based NAO-index version (Hurrell et al. 2003), because it offers the tightest correlations with Estonian storminess, sea level and wave data (Jaagus & Suursaar 2013). Finally, some background data on wind and wave climates of the Estonian coastal sea were used (Suursaar 2015; Suursaar et al. 2015).

Table 2. Detailed description of the patterns along specific profile sections within the longer transects (shown in bold in Table 1). AUR, apparent uplift rate in the late Holocene ($AUR = LU(G) - 0.2$, mm/yr); Alt R, altitude range (m); Alt S, altitude span (m); HDR, horizontal distance range on the profile (m); L, length of the section (m); Age R, age range (cal yr BP – years before present; Age = altitude/AUR); Age S, age span (yr); SS, spatial spacing, metres per ridges ($SS = L/\text{ridges}$); TS, time spacing, years per ridges ($TS = \text{Age R}/\text{ridges}$). Note that the cyclicity estimation (TS) is based on relative age differences (age spans), the ages are calculational and should not be taken as exact absolute ages

Section	AUR	Alt R	Alt S	HDR	L	Age R	Age S	Ridges	SS	TS
1a	3.2	4.4–7.1	2.7	115–985	870	1375–2219	844	37	24	23
3a	3.2	6.2–7.9	1.7	1090–1490	400	1938–2469	531	21	19	28
4a	3.1	9.2–12.2	3.0	330–1020	690	2968–3935	967	29	24	33
5a	3.1	2.3–6.5	4.2	20–1140	1120	742–2097	1355	44	25	31
5b	3.1	8.8–13.5	4.7	1640–2920	1280	2839–4355	1516	49	26	31
6a	3.0	3.2–6.2	3.0	190–940	750	1067–2067	1000	37	20	27
6b	3.0	9.8–12.3	2.5	1930–2620	690	3267–4100	833	27	26	31
7a	3.0	5.2–13.5	8.3	800–3200	2400	1733–4500	2767	85	28	33
8a	2.9	6.5–11.9	5.4	20–1020	1000	2241–4103	1862	48	21	39
16a	2.9	4.2–9.6	5.4	0–1300	1300	1448–3310	1862	49	27	38
Average									24	31

Counting the ridges and characterization of patterns

A large number of geomorphic features with different height and spacing can be identified from LiDAR images (Fig. 4) and height profiles (Fig. 5). A persistent regularity of elevated shore patterns can be seen at many sections. We calculated the average spatial and temporal spacings of ridges over the selected profiles by dividing the number of ridges either by the length of the section or by the age difference within the profile, respectively (Table 2).

Counting ridges involves some subjectivity, as no software exists for that purpose. A profile of the shore emerging from the sea is never perfectly linear. Varying conditions lead to a distinct character of each profile. While counting ridges from the shore profiles, we normally did not treat as a ridge a feature with a height below 20 cm unless a sequential pattern suggested otherwise. We usually took two readings: one that considered some smaller features as ‘ridges’, and another that excluded such smaller features. The difference between those readings was usually less than 10%. Table 2 shows the averages for each of the profile sections. Occasionally, the presence of roads, ditches, settlements or fields further complicated the counting of ridges in the shore profiles. In order to exclude these features, some of the profiles were divided into two sections (a and b, Table 2). We note that the exact ages (in Table 2) were not verified by other dating methods, and they should be taken as approximations only. It would be a huge task to get carbon-14, optically stimulated luminescence or other kind of numerical dating for each individual landscape feature. Our method for describing cyclicity rather works on the basis of age differences over cross sections and some descriptive statistics.

Although occasionally expressing some fine patterns (e.g. Fig. 5F, 3200–4200 m; Fig. 5H, 1200–2700 m; Fig. 5J, 2400–3200 m), the portions of the shore profiles lying in elevations above 14 m were excluded in this analysis. One reason is that smaller features tend to get lost over time (i.e., eroded or anthropogenically rearranged) and counting ridges under such circumstances may lead to erroneous estimates. Secondly, the relative sea level lowering curve is not known with acceptable accuracy. As it was mentioned before, the period before 7500 yr BP included some dramatic, eustatic sea level variations due to glacial melting with time-varying rates, tectonic uplift and glacial isostasy (Muru et al. 2017). The period between 7500 and 4500 yr BP probably included some non-linear changes in eustatic sea level rise as well (Lambeck et al. 2014). These profile sections can be analysed in future, when improved sea level reconstructions become available.

We assume that the results of our cyclicity calculations are confident within the $\pm 20\%$ limits, since the ingredient factors (uplift, sea level rise, ridge counting) are approximations, too, with inherent accuracies of about $\pm 5\text{--}10\%$ (e.g. Vassiljev et al. 2015; Santamaría-Gómez et al. 2017).

RESULTS AND DISCUSSION

Description of the ridge patterns

Even if some large sections above 14 m with obvious ridge patterns are excluded, there are plenty of recent and rather clear patterns at altitudes below 14 m a.s.l. (or less than approximately 4500 years old), some of which populate ridge plains up to 4 km inland (Fig. 4).

The heights of the ridges were typically between 0.2 and 1 m, and in some cases, up to 2 m, but according to surveys using GPRs (Vilumaa et al. 2016), the internal amplitude of partly buried ridges can be even higher. The selected sections (Table 2) can be seen in Fig. 5. Disrupted by a dune belt, profile No. 2 can be viewed in Vilumaa et al. (2016). It seems that the dune belt overrides the older coastal formations and aeolian accretion may have changed the height of the ridges there. The same dune belt can be found in many northerly exposed coastal sections of Estonia. The base of the dune belt is 4–5 m a.s.l. and its relative height reaches 10 m in the Tahkuna and Lõimastu–Lehtma area (Figs 4, 5). The age of this dune is estimated at about 1200 years, but its exact formation mechanism is not known. Various theories include extreme events such as a massive ice attack, tsunami or intense aeolian activity during a period of windy and cold climates (Anderson et al. 2014; Vilumaa et al. 2017).

The most extensive ridge systems can be found in the Lehtma–Tareste–Kanapeeksi region. Approximately 4 km long cross-shore sections can be found along 10 km wide coastal expanses and over a hundred regularly spaced ancient coastal ridges can be counted in that area (Figs 4A, B, 5). In fact, Table 2 shows only some of the possible examples there. The same applies to the Mänspe–Õngu region (Figs 4C, 5). Adding up the ridges over individual sections along up to 4 km long transects yields 119–137 ridges at Tareste, 144–170 at Kanapeeksi and 87–102 at Õngu. Outside Hiiumaa Island, some spectacular, unspoiled examples can be found on Osmussaar Island and in the Nõva–Keibu region (Fig. 5J, K). At the southeastern tip of Osmussaar Island, 14–15 m spaced stripes are visually identifiable (e.g. on aerophotographs) by contrasting vegetation (Fig. 2). The high regularity of ridges on Osmussaar can be explained by rough limestone material (pebbles, shingles) that is slowly eroding from the NE side of the island (Suursaar et al. 2013), and the relatively fast postglacial uplift, which enables the preservation of the older ridges. The ridge material can be of various grain sizes from medium sand to gravel and even to boulders. The origin can be moraine from some of the glacial episodes, coastal and marine deposits (assorted sands, pebbles, cobbles, boulders), or bedrock material from the seafloor and nearby cliffs and transported by waves (Orviku 1974; Tõnissou et al. 2014).

The spacing of ridges in the ridge systems analysed varied between 19 and 28 m (with a gross-average of 24 m, standard deviation 3.1 m). The average temporal periodicity of the ridges was 23–39 years (Table 2), while the gross-average was 31.4 years with a standard deviation of 4.8 years. Calculating gross-averages is justified, since the study sites belong to similar uplift

and met-ocean forcing conditions. It enables generalized and statistically more stable results.

The crest-to-crest spacing seems to be a bit shorter (with somewhat steeper profiles) where the ridges are composed of relatively coarser material, and longer where sandy material predominates. However, the temporal spacing was rather consistent and the relationship between spatial and temporal spacing was weak. Somewhat shorter temporal spacing (23–31 years) mainly coincided with younger cross sections, while upper sections yielded somewhat longer periodicity (31–39 years). The average periods in the patterns were still quite similar (23–39 years) among the Estonian study sites (Table 2). Considering that the geomorphic process is merely quasi-periodical and by no means deterministic, the differences are not significant. The differences can be explained by age, the influence of local topographic features, variations in the coastal slope (as seafloor emerges) and changes in sediment supply. For example, some ridges may be buried by peat, or material from older (weaker) ridges may be recycled into new ridges. Any of these occurrences may cause so-called ‘data reversals’ during the counting.

The relative consistency of results in the study area can be explained by the location of the ridge patterns in the same sea area, resulting in similar forcing conditions and uplift rate. According to the global overview by Scheffers et al. (2012), the spacing of beach ridges (ranging from 6 to 800 m) may be very irregular from site to site, but more regular within the same transect. Temporal periodicity varied between 15 and 300 years, and therefore it was difficult to pinpoint one dominating period or mechanism. However, as opposed to areas in the tropics or southern hemisphere, the prevalence of shorter periods (15–60 years) has been mentioned at Spitsbergen, Alaska, Norway and Denmark (Brückner et al. 2002; Nielsen et al. 2006), all of which lie in regions influenced by the NAO.

Because the periodicity in Estonia was more or less uniform for the whole of the study region, it could coincide with some kind of periodicity in external forcing. An alternative explanation could be that the period is entirely or partly determined by a combination of the morphological features such as grain size, apparent uplift rate, slope and wave energy.

Ridge pattern formation mechanisms

Although forcing conditions are mostly mild or moderate in the Baltic Sea and wind direction is variable, Estonian seacoasts are, for a variety of reasons, uniquely suited for the development of patterned beach ridge formations. According to numerous papers on beach ridges, a set of factors such as wave forcing, the availability of

appropriate building materials, slope topography and certain sea level phenomena are important (Buscombe & Masselink 2006; Hayes et al. 2010). However, most of these studies were carried out on coasts with considerable tidal influence. The ridge formation mechanisms can be somewhat different on the east coast of the Baltic Sea, a non-tidal area known for its storms and land uplift. According to our analysis (Table 1), the rhythmic ridge systems were mainly found on gently sloping, well-exposed western and northern coasts of Estonia (Fig. 1) known for its relatively quicker uplift rates (2.7–3.4 mm/yr). They were rare in the Väinameri Sea, as well as along the coasts of the Gulf of Riga, where just some faint structures can be found near Tõstamaa, as well as on Ruhnu Island and along the eastern coast of the Sõrve Peninsula. It seems that owing to small wave fetches (Suursaar 2015), the hydrodynamic forcing is not enough for building up considerable beach ridge systems there (even though aeolian landforms are still present). Also, the land uplift rate is smaller there and the present sea level is already slightly increasing according to the tide gauge data in Pärnu (Jaagus & Suursaar 2013) and Narva-Jõesuu (Fig. 6). Slow uplift or land subsidence is

more favourable for dune formation as the shoreline position is stable for a long time. Finally, a replacement of morainic, limestone-dominated and mixed (sand and gravel) coasts in Northwest Estonia by fine-grained sandy shores in the south can be observed. Fine sand is not a good material for the preservation of shore-parallel ridges. It has to be populated by vegetation quickly and isolated from the destructive coastal processes, which is only possible in case of fast uplift. Aeolian processes can modulate or stress the newly formed ridge patterns, create ‘aeolian caps’ to the ridges (Vilumaa et al. 2017) or even override them. But aeolian processes cannot serve as the primary building mechanisms for the ridge systems under this study, as the existing shore-parallel ridges are too regular and continuous over long sequences, and their uninterrupted, gentle curving patterns differ considerably from the typical patterns of dunes and foredunes.

Two subtypes of ridge formation mechanisms can be drawn, one for sand-dominated coasts and the other for coarser material, pebbles and cobbles. Sand-based ridges have formed as a result of the combination of accumulation and shape-enhancing erosion, repeated over periods of time. Sand is gradually accumulating on the

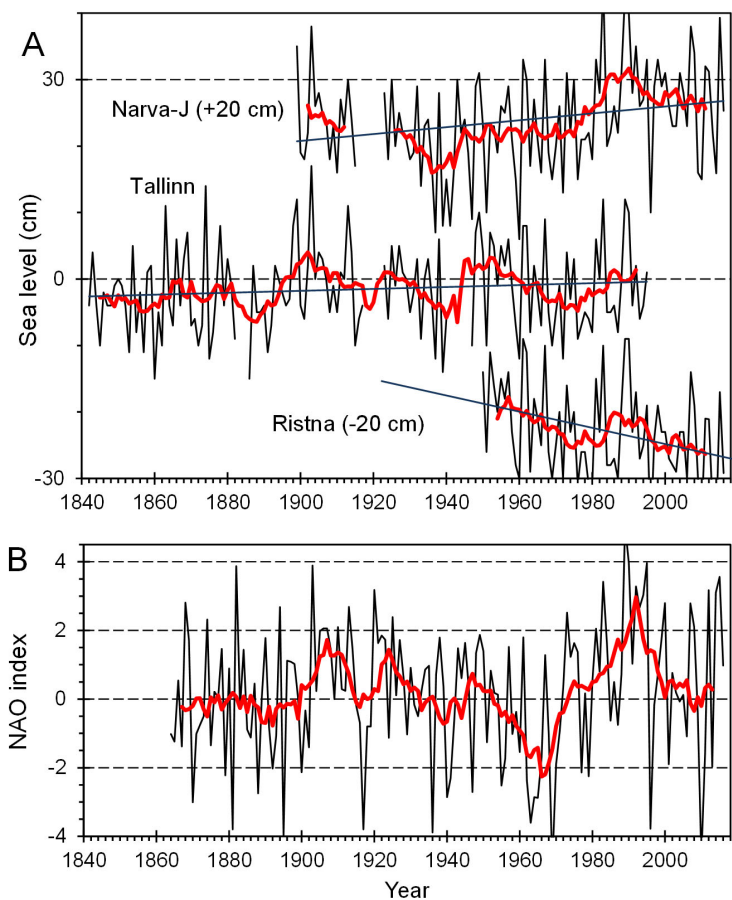


Fig. 6. Relative sea level variations at three tide gauges (Narva Jõesuu shifted for +20 cm and Ristna –20 cm) together with their 9-year moving averages, expressing a weak periodicity (A). Hurrell station-based (DJFM) NAO-indices with 9-year moving averages (B) (<https://climatedataguide.ucar.edu/>).

backshore due to aeolian and wave activity, while storms wash those accumulative forms periodically, forming a distinctive scarp at a specific elevation (Tõnisson et al. 2013). In a quieter phase of storm activity or after an extreme storm, the erosional scarp will be left alone on the higher ground. Wave activity is lower during such periods and does not reach the scarp any more, and accumulation as well as subsequent erosional episodes shift seawards. Finally, old scarp becomes somewhat smoothed or denudated by aeolian processes and covered by vegetation (Vilumaa et al. 2016), while younger features are gradually formed seawards. It also seems that the influx of sediment must occur at appropriately consistent and low levels. Movable sand that arrives in large amounts at the same time may lead to the formation of dunes and not beach ridge systems.

The formation and preservation of beach ridge systems is more straightforward in the case of coarse or morainic material, as it is not easy to relocate during each storm-wave event. Unlike sandy deposits, gravel and pebble deposits gradually form the same ridge, reinforcing or elongating the existing ones (Tõnisson et al. 2014; Suursaar et al. 2015). The repeated ridge formation process usually involves both longshore sediment transport and gradual cross-shore pile-up of the material. The erosion of hard sediments from nearby cliffs, headlands or the sea bottom is slow but fairly constant. Relatively strong waves are needed to move coarser material against gravity to build up ridges. Uprush is quicker than down-wash and material is thrown on top of the berm up to the height of the swash surge (Nott et al. 2015). Short-term sea level variations may enhance the effect of wave activity during storms, but long-term sea level variation is still a crucial factor for beach ridge development (Buynevich et al. 2007). While rising sea level promotes erosion and sediment relocation, deactivation and preservation of beach ridge systems occur in cases of relative sea level fall.

Although single, new beach ridges could be formed during one or two extreme storm events (Tõnisson et al. 2013), the physical effects of individual storms typically disappear within a few decades, as new material is piled up onto a stronger ridge. Such a gradual pile-up is favoured by a longer period of elevated storminess (Allard et al. 2008). If storminess recedes, the new material cannot be added on top of the ridge. It populates new, relatively small ridges between the shoreline and the old, large ridge. When the storminess increases again, those small ridges will be pushed together, forming a protective barrier between storm waves and the old ridge. As a result, a new high ridge is formed just seawards from the previous ridge. The decadal variations in storminess (Suursaar et al. 2015) ought not to be too substantial in order to create periodicity in beach deposits.

Indeed, if the swash height during storms becomes 10 cm short (which can also be a result of e.g. 30 years of land uplift with a rate of 3 mm/yr), it starts to contribute to the distancing of the ridge from the sea. Even if some of the storms may reach the old crest, others routinely widen the gap and finally trigger a shift in the build-up system. The gap also widens on account of coarser material, which cannot be moved on top of the ridge. Basically, when the gap between shoreline and the previous large ridge becomes too wide and the ridge behind is too high, the next beach ridge starts to grow seawards. Uplift transports the gradually added features to a higher elevation and out of reach of transforming littoral processes.

Possible reasons for periodicity

Since beach ridge systems exhibit certain step-like processes and rhythmic impacts over long periods, it is important to find out whether a kind of corresponding periodicity in forcing conditions exists. First of all, seasonality occurs in storm-wind conditions, sea level variations and wave heights (Jaagus & Suursaar 2013; Suursaar 2015). Extreme storms, on the other hand, happen irregularly and randomly, even though the occurrence statistics are usually expressed in a manner that mimics periodicity (e.g. ‘once in a decade storm’). Considering the quasi-regular ~31-year periodicity (Table 2) of the ancient coastal ridges on the Estonian study sites, the immediate forcing can neither be seasonality nor isolated, extreme storm events.

Still, a suitable, decadal-scale variation in general storminess exists in the region of the Baltic Sea (Fig. 6A). Indeed, a quasi-regular 25–40-year periodicity can be seen in Estonian sea level records, especially after a smoothing procedure with a moving average. Since 1840, five to six cycles have been identified (Fig. 6A), which yields a mean period of 29–35 years. Similarly-phased cycles also occur in wave conditions (Suursaar et al. 2015), which is another important forcing for beach ridges, as well as in local expressions of storminess (i.e. count of storm days; Suursaar et al. 2015). Thus, on top of the weak (~30-year) periodicity in sea level, there is also a similarly phased (weak) periodicity in winds, waves and currents, which all together seem to magnify their impact on the windward-located coasts of Estonia (Suursaar & Kullas 2006). Quite similar cyclicity has also been described in some other (and somewhat longer) climate-related time series in Estonia. For instance, a reconstruction of precipitation by Tarand et al. (2013) includes nine highs and eight lows since 1750 (Fig. 7), which yields an average period of approximately 30 years. The decadal-scale variations in most of the mentioned factors are more or less synchronous to each other

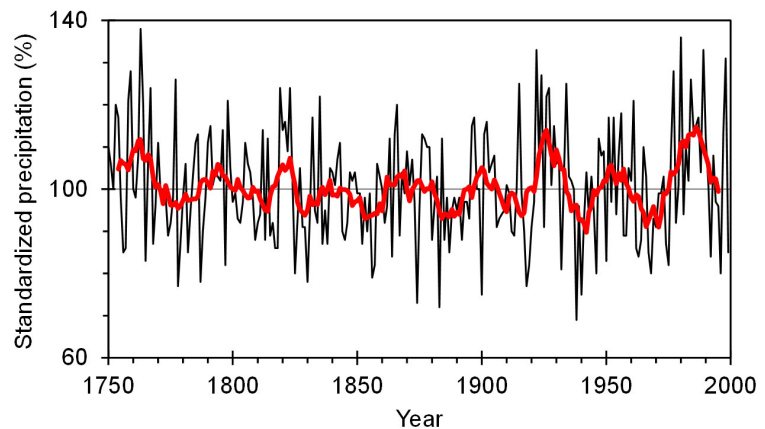


Fig. 7. Reconstruction of annual sums of relative precipitation amounts together with 9-year running averages in Estonia (according to data presented in table 4.2.3, Tarand et al. 2013).

mainly because they all seem to have a more general, common cause, which, in turn, seems to be connected to the NAO in Estonia (Fig. 6B). Close correlation between the NAO index, sea level variations, precipitations and wind conditions is widely acknowledged in the Baltic Sea area (Jaagus & Suursaar 2013; Johansson & Kahma 2016). However, the causes of periodicity in the NAO itself and its further connections to other climate phenomena are not so clear (Hurrell et al. 2003).

Although the periodicity of ancient coastal ridges and the periodicity in possible forcing seem to match well, neither of these processes is exactly sinusoidal. Also, it is not easy to define the specific underlying mechanism. It has been a frustration in various studies that any deterministic connections between erosion/accumulation quantities and immediate forcing conditions, such as storm or wave parameters, sea level height, etc., hardly exist (Orviku et al. 2009; Suursaar et al. 2016). The correlative relations have been varying among study sites, and by no means are suitable for extrapolation. It means that we could not directly simulate the sequential increments of masses in beach ridge systems depending on the historic variations in wave conditions or the NAO.

Cyclic development in beach ridges may occur (or be stressed) through shifts in a self-organizing system. The energy of the event initiating a shift to a new ridge build-up does not have to be prominent. A shift rather appears when certain preconditions regarding sediment accretion and uplift are reached and a kind of self-regulatory mechanism may help to select a suitable periodicity from the time-varying forcing. We hypothesize that the process could have a formal similarity to oscillatory resonance processes, which is common in the nature (e.g. Otsmann et al. 2001). The physical features of the specific coastal geomorphic system (which probably includes uplift rate, slope and sediment properties) determine a possible periodicity range for the shift. An available external forcing with the closest

period is selected (picked up) just like a self-oscillation frequency is revealed under time-varying external forcing by a pendulum. The exact range of suitable periods is unknown, but in our case, the ~ 30 -year cyclicality in the NAO is both suitable and present in the North Atlantic region. We admit that in other parts of the world, a different kind of decadal-scale quasi-periodicity or forcing mechanisms may be present. We also accept that some ridges may be created by aperiodic or single, random extreme storms (Nott et al. 2015) and some ridges might be merged by such extreme and rare events. We also hypothesize that even annual (seasonal) ridge spacing could be in principle possible, but the uplift must be much (10–30 times) faster than and also the deliverance of adequate sediment quantities should exist.

The question arises: How can we be sure that this kind of periodicity has existed over several thousands of years in order to produce more than 100 ridges? The periodicity in the NAO index is usually described as having a weak cyclic pattern where roughly a 30–40-year cycle shows up in terms of a moving average (Fig. 6B). Another important cyclic mechanism seems to be the Atlantic Meridional Overturning Circulation (Cronin et al. 2014). Based on early instrumental data, the NAO has been extended back to 1825 (Jones et al. 1997), accommodating 5–6 cycles. It is prone to ‘phase reversals’ (one occurred around 1900), which distorts (lengthens or shortens) the possible periodicity estimates. A 600 years long NAO reconstruction by Olsen et al. (2012) includes an approximate 30-year periodicity and 60-year periodicity (which can be harmonically linked to a 30-year period). The Fourier analysis of the palaeo sea level curve over the last 2000 years performed by Cronin et al. (2014) exhibited, aside from the peaks at 185 and 21 years, a significant peak at 31 years (29.9–32.9 years). Such quasi-regular processes have often been explained by some external, more general forcing (Landscheidt 1988; Zanchettin et al. 2008). For

instance, Theodore Landscheidt was convinced that the NAO and El Niño–Southern Oscillation, as well as Pacific Decadal Oscillations, were all closely linked to the Sun’s eruptional activity, 16-year torque cycle and the so-called solar perturbation cycle with a mean length of 35.8 years. Actually, there is a large number of various planetary cycles present, and it is not well understood how they interact, combine or manifest themselves in various parts of the Earth’s system (Zanchettin et al. 2008). The connection of processes like the NAO with certain deterministic or periodic, planetary or solar processes is very tempting, since it could provide an opportunity to predict climatic variations in the future. However, even if we may assume that a kind of climatic decadal-scale variability continues to exist, the future of the beach ridge systems may be questionable under global sea level rise (Church et al. 2013), which firstly hinders the ridge-formation mechanisms and then begins to destroy the existing ones.

SUMMARY AND CONCLUSIONS

A large number of rhythmic geomorphic patterns were found from LiDAR images and high-resolution elevation data on the non-tidal seacoasts of Estonia subject to postglacial uplift. These have been characterized as elevated, old beach ridge or coastal scarp systems. Twenty-seven areas, up to 5–10 km inland from the contemporary coastline, were examined in this study, and ten of them were reviewed in greater detail for discussing possible formation mechanisms and periodicity in the patterns. The clearest rhythmic ridge systems were mainly found on gently sloping, well-exposed western and northern coasts with quicker uplift rates (2.7–3.4 mm/yr) and adequate sediment supply.

The origin of the ridge material could be moraine (mainly from the latest glacial episode), coastal and marine deposits (sorted sands, pebbles, cobbles, boulders), or bedrock material worked out by waves from the seafloor and nearby cliffs. Although it is sometimes difficult to find out the main forming factor for the sand-built rhythmic patterns – is it either wind or hydrodynamic agents (waves, sea level variations, currents) – the aeolian processes alone cannot serve as the primary building mechanisms for the highly regular, continuous and gently curving ridge systems. The rhythmic patterns must either be formed as consecutive ridges or elevated (partly denudated), parallel coastal scarps. In future studies, differentiation between these sub-types and ridge material sources should be made.

Approximately 150 individual ridges were counted on up to 4 km long cross-shore sections. Based on the height difference over the selected (less than ~4500

years old) sections and late Holocene apparent land uplift rates of each location, the corresponding time spans, as well as mean crest-to-crest temporal spacings, were calculated. The mean period in the ridge systems was estimated as 31 years; the mean ridge spacing varied between 19 and 28 m. Considering the relatively long periods and the regular nature of the ridges, they neither reflect seasonal storminess nor single extreme storms or tsunamis, but rather a decadal-scale periodicity in large-scale storminess. They can be linked with the quasi-periodic 25–40-year variability, which can be found in Estonian long-term sea level records and wave hindcasts, as well as in regional storminess indices and the NAO. However, neither the cyclicity in ridge patterns nor the cyclicity in the forcing are sinusoidal. Some kind of self-organizing sediment accumulation mechanisms could be present, which reveals a suitable periodicity from the existing, time-varying met-ocean forcing and enhances its effect through repeated shifts in beach ridge formation.

In the case of sandy shores, the periodic process involves initial accumulation and sandy ridge formation, then, the formation of shape-enhancing erosional scarp and finally its smoothening and vegetation on a higher ground, while new ridges are formed seawards. In the case of accumulated, gravel-pebble shores, a reinforcement and gradual pile-up of a fresh ridge occurs over a period of elevated storminess (which, as a composite forcing, includes synchronously working impacts of sea level variations, waves, currents and winds). If storminess recedes, the new material cannot be added on top of the ridge; it rather populates the berm on the base of the ridge. As a combined result of uplift and accumulation, either the gap becomes too wide or the ridge gets too high, so the next beach ridge starts to grow seawards. Very much like a conveyor belt, uplift transports the gradually added material (or previous scarp) to a higher elevation. While ridge systems are gradually ‘archived’ and placed out of reach of transforming littoral processes at neotectonically or glacio-isostatically uplifting coasts, the anticipated acceleration of global sea level rise firstly hinders the ridge-formation mechanisms and then begins to destroy the existing ones.

Acknowledgements. The study was supported by the project IUT18-9 of the Estonian Ministry of Education and Research, and the Estonian Research Council grant PUT1439. We thank the Estonian Land Board for providing elevation data and the Estonian Environmental Agency for sea level data. We are grateful to K. Furmańczyk and the anonymous reviewer for thorough and fruitful remarks, which helped to improve the manuscript. The publication costs of this article were partially covered by the Estonian Academy of Sciences.

REFERENCES

- Allard, J., Bertin, X., Chaumillon, E. & Pouget, F. 2008. Sand spit rhythmic development: a potential record of wave climate variations? Arcay Spit, western coast of France. *Marine Geology*, **253**, 107–131.
- Anderson, A., Vilumaa, K., Tõnisson, H., Kont, A., Ratas, U. & Suuroja, S. 2014. Geomorphology of coastal formations on present and ancient sandy coasts. *Journal of Coastal Research*, Special Issue, **70**, 90–95.
- Brückner, H., Schellmann, G. & van der Borg, K. 2002. Uplifted beach ridges in northern Spitsbergen as indicators for glacio-isostasy and palaeo-oceanography. *Zeitschrift für Geomorphologie*, NF, **46**, 309–336.
- Buscombe, D. & Masselink, G. 2006. Concepts in gravel beach dynamics. *Earth-Science Reviews*, **79**, 33–52.
- Buynevich, I. V., FitzGerald, D. M. & Goble, R. J. 2007. A 1500 yr record of North Atlantic storm activity based on optically dated relict beach scarps. *Geology*, **35**, 543–546.
- Church, J. A., Clark, P. U., Cazenave, A., Gregory, J. M., Jevrejeva, S., Levermann, A., Merrifield, M. A., Milne, G. A., Nerem, R. S., Nunn, P. D., Payne, A. J., Pfeffer, W. T., Stammer, D. & Unnikrishnan, A. S. 2013. Sea level change. In *Climate Change 2013: The Physical Science Basis. Contribution of Working Group I to the Fifth Assessment Report of the Intergovernmental Panel on climate Change* (Stocker, T. F., Qin, D., Plattner, G.-K., Tignor, M., Allen, S. K., Boschung, J., Nauels, A., Xia, Y., Bex, V. & Midgley, P. M., eds), pp. 1137–1216. Cambridge University Press, Cambridge, United Kingdom and New York.
- Cronin, T. M., Farmer, L., Marzen, R. E., Thomas, E. & Varekamp, J. C. 2014. Late Holocene sea level variability and Atlantic Meridional Overturning Circulation. *Paleoceanography*, **29**, 765–777.
- Ekman, M. 1996. A consistent map of the postglacial uplift of Fennoscandia. *Terra Nova*, **8**, 158–165.
- Furmańczyk, K. K., Dudzińska-Nowak, J., Furmańczyk, K. A., Papińska-Swerpel, B. & Brzezowska, N. 2011. Dune erosion as a result of the significant storms at the western Polish coast (Dziwnow Spit example). *Journal of Coastal Research*, Special Issue, **64**, 756–759.
- Grudzinska, I., Saarse, L., Vassiljev, J. & Heinsalu, A. 2013. Mid- and late-Holocene shoreline changes along the southern coast of the Gulf of Finland. *Bulletin of the Geological Society of Finland*, **85**, 19–34.
- Gruno, A., Liibus, A., Ellmann, A., Oja, T., Vain, A. & Jürgenson, H. 2013. Determining sea surface heights using small footprint airborne laser scanning. In *Proceedings SPIE 8888, Remote Sensing of the Ocean, Sea Ice, Coastal Waters, and Large Water Regions 2013*, 88880R (October 16, 2013).
- Hayes, M., Michel, J. & Betenbaugh, D. 2010. The intermittently exposed, coarse-grained gravel beaches of Prince William Sound, Alaska: comparison with open-ocean gravel beaches. *Journal of Coastal Research*, **26**, 4–30.
- Hurrell, J. W., Kushnir, Y., Ottersen, G. & Visbeck, M. 2003. An overview of the North Atlantic Oscillation. In *The North Atlantic Oscillation – Climatic Significance and Environmental Impact* (Hurrell, J. W., Kushnir, Y., Ottersen, G. & Visbeck, M., eds), *Geophysical Monograph Series*, **134**, 1–35.
- Jaagus, J. & Suursaar, Ü. 2013. Long-term storminess and sea level variations on the Estonian coast of the Baltic Sea in relation to large-scale atmospheric circulation. *Estonian Journal of Earth Sciences*, **62**, 73–92.
- Johansson, M. & Kahma, K. K. 2016. On the statistical relationship between the geostrophic wind and sea level variations in the Baltic Sea. *Boreal Environment Research*, **21**, 25–43.
- Jones, P. D., Jónsson, T. & Wheeler, D. 1997. Extension to the North Atlantic Oscillation using early instrumental pressure observations from Gibraltar and South-West Iceland. *International Journal of Climatology*, **17**, 1433–1450.
- Kall, T., Liibus, A., Wan, J. & Raamat, R. 2016. Vertical crustal movements in Estonia determined from precise levellings and observations of the level of Lake Peipsi. *Estonian Journal of Earth Sciences*, **65**, 27–47.
- Kessel, H. & Raukas, A. 1967. *The Deposits of Ancylus Lake and Littorina Sea in Estonia*. Valgus, Tallinn, 134 pp. [in Russian, with English summary].
- Lambeck, K., Woodroffe, C. D., Antonioli, F., Anzidei, M., Gehrels, W. R., Laborel, J. & Wright, A. J. 2010. Paleo-environmental records, geophysical modelling, and reconstruction of sea level trends and variability on centennial and longer timescales. In *Understanding Sea Level Rise and Variability* (Church, J. A., Woodworth, P. L., Aarup, T. & Wilson, W. S., eds), pp. 61–121. Wiley-Blackwell, Hoboken, NJ, USA.
- Lambeck, K., Rouby, H., Purcell, A., Sun, Y. & Sambridge, M. 2014. Sea level and global ice volumes from the Last Glacial Maximum to the Holocene. *Proceedings of the National Academy of Sciences of the United States of America*, **111**, 15296–15303.
- Landscheidt, T. 1988. Solar rotation, impulses of the torque in the Sun's motion, and climatic variation. *Climatic Change*, **12**, 265–295.
- Muru, M., Rosentau, A., Kriiska, A., Lõugas, L., Kadakas, U., Vassiljev, J., Saarse, L., Aunap, R., Küttim, L., Puusepp, L. & Kihno, K. 2017. Sea level changes and Neolithic hunter-fisher-gatherers in the centre of Tallinn, southern coast of the Gulf of Finland, Baltic Sea. *Holocene*, **27**, 917–928.
- Nielsen, A., Murray, A., Pejrup, M. & Elberling, B. 2006. Optically stimulated luminescence dating of a Holocene beach ridge plain in Northern Jutland, Denmark. *Quaternary Geochronology*, **1**, 305–312.
- Nott, J. 2004. Palaeotempestology: the study of prehistoric tropical cyclones – a review and implications for hazard assessment. *Environment International*, **30**, 433–447.
- Nott, J., Forsyth, A., Rhodes, E. & O'Grady, D. 2015. The origin of centennial- to millennial-scale chronological gaps in storm emplaced beach ridge plains. *Marine Geology*, **367**, 83–93.
- Olsen, J., Anderson, N. J. & Knudsen, M. F. 2012. Variability of the North Atlantic Oscillation over the past 5200 years. *Nature Geoscience*, **5**, 808–812.
- Orviku, K. 1974. *Seacoasts of Estonia*. Tallinn, 112 pp. [in Russian, with English summary].

- Orviku, K., Suursaar, Ü., Tõnisson, H., Kullas, T., Rivis, R. & Kont, A. 2009. Coastal changes in Saaremaa Island, Estonia, caused by winter storms in 1999, 2001, 2005 and 2007. *Journal of Coastal Research*, Special Issue, **56**, 1651–1655.
- Otsmann, M., Suursaar, Ü. & Kullas, T. 2001. The oscillatory nature of the flows in the system of straits and small semienclosed basins of the Baltic Sea. *Continental Shelf Research*, **21**, 1577–1603.
- Raukas, A. & Hyvärinen, H. (eds). 1992. *Geology of the Gulf of Finland*. Valgus, Tallinn, 422 pp. [in Russian, with English summary].
- Rivis, R. 2004. Changes in shoreline positions on the Harilaid Peninsula, West Estonia, during the 20th century. *Proceedings of the Estonian Academy of Sciences, Biology, Ecology*, **53**, 179–193.
- Saarse, L., Vassiljev, J., Rosentau, A. & Miidel, A. 2007. Reconstructed late glacial shore displacement in Estonia. *Baltica*, **20**, 35–45.
- Santamaría-Gómez, A., Gravelle, M., Dangendorf, S., Marcos, M. & Wöppelmann, G. 2017. Uncertainty of the 20th century sea-level rise due to vertical land motion errors. *Earth and Planetary Science Letters*, **473**, 24–32.
- Scheffers, A. & Scheffers, S. 2006. Documentation of the impact of Hurricane Ivan on the coastline of Bonaire (Netherlands Antilles). *Journal of Coastal Research*, **22**, 1437–1450.
- Scheffers, A., Engel, M., Scheffers, S., Squire, P. & Kelletat, D. 2012. Beach ridge systems: archives for Holocene coastal events? *Physical Geography*, **36**, 5–37.
- Simpson, M. J. R., Nilsen, J. E. Ø., Ravndal, O. R., Breili, K., Sande, H., Kierulf, H. P., Steffen, H., Jansen, E., Carson, M. & Vestøl, O. 2015. *Sea Level Change for Norway: Past and Present Observations and Projections to 2100*. Norwegian Centre for Climate Services report 1/2015. Oslo, Norway, 156 pp.
- Suursaar, Ü. 2015. Analysis of wave time series in the Estonian coastal sea in 2003–2014. *Estonian Journal of Earth Sciences*, **64**, 289–304.
- Suursaar, Ü. & Kall, T. 2017. Interpretation of relative sea level variations at tide gauges using results from four Estonian precise levellings and land uplift models. In *IEEE International Geoscience and Remote Sensing Symposium (IGARSS), 23–28 July 2017, Fort Worth, Texas, USA*, pp. 6000–6003. IEEE.
- Suursaar, Ü. & Kullas, T. 2006. Influence of wind climate changes on the mean sea level and current regime in the coastal waters of west Estonia, Baltic Sea. *Oceanologia*, **48**, 361–383.
- Suursaar, Ü., Tõnisson, H., Kont, A. & Orviku, K. 2013. Analysis of relationships between near-shore hydrodynamics and sediment movement on Osmussaar Island, western Estonia. *Bulletin of the Geological Society of Finland*, **85**, 35–52.
- Suursaar, Ü., Jaagus, J. & Tõnisson, H. 2015. How to quantify long-term changes in coastal sea storminess? *Estuarine, Coastal and Shelf Science*, **156**, 31–41.
- Suursaar, Ü., Tõnisson, H., Alari, V., Raudsepp, U., Rästas, H. & Anderson, A. 2016. Projected changes in wave conditions in the Baltic Sea by the end of 21st century and the corresponding shoreline changes. *Journal of Coastal Research*, Special Issue, **75**, 1012–1016.
- Tamura, T. 2012. Beach ridges and prograded beach deposits as palaeoenvironment records. *Earth-Science Reviews*, **114**, 279–297.
- Tarand, A., Jaagus, J. & Kallis, A. 2013. *Eesti kliima minevikus ja tänapäeval [Estonian Climate; Past and Present]*. University of Tartu Publishers, Tartu, 631 pp. [in Estonian].
- Taylor, M. & Stone, G. W. 1996. Beach-ridges: a review. *Journal of Coastal Research*, **12**, 612–621.
- Tõnisson, H., Suursaar, Ü., Rivis, R., Kont, A. & Orviku, K. 2013. Observation and analysis of coastal changes in the West Estonian Archipelago caused by storm Ulli (Emil) in January 2012. *Journal of Coastal Research*, Special Issue, **65**, 832–837.
- Tõnisson, H., Suursaar, Ü., Kont, A., Orviku, K., Rivis, R., Szava-Kovats, R., Vilumaa, K., Aarna, T., Eelsalu, M., Pindsoo, K., Palginõmm, V. & Ratas, U. 2014. Field experiments with different fractions of painted sediments to study material transport in three coastal sites in Estonia. *Journal of Coastal Research*, Special Issue, **70**, 229–234.
- Torim, A. 2004. About the land uplift and variation of the coastline in Estonia. *Geodeet*, **28**, 57–62.
- Vallner, L., Sildvee, H. & Torim, A. 1988. Recent crustal movements in Estonia. *Journal of Geodynamics*, **9**, 215–223.
- Vassiljev, J., Saarse, L., Grudzinska, I. & Heinsalu, A. 2015. Relative sea level changes and development of the Hiiumaa Island, Estonia, during the Holocene. *Geological Quarterly*, **59**, 517–530.
- Vestøl, O., Ågren, J., Steffen, H., Kierulf, H., Lidberg, M., Oja, T., Rüdja, A., Kall, T., Saaranen, V., Engsager, K., Jepsen, C., Liepins, I., Paršeliūnas, E. & Tarasov, L. 2016. NKG2016LU, an improved postglacial land uplift model over the Nordic-Baltic region. Presentation at Nordic Geodetic Commission Working Group of Geoid and Height Systems meeting, Tallinn, 12–18 March 2016.
- Vilumaa, K., Tõnisson, H., Sugita, S., Buynevich, I. V., Kont, A., Muru, M., Preusser, F., Bjursäter, S., Vaasma, T., Vandel, E., Molodkov, A. & Järvelill, J. I. 2016. Past extreme events recorded in the internal architecture of coastal formations in the Baltic Sea region. *Journal of Coastal Research*, Special Issue, **75**, 775–779.
- Vilumaa, K., Ratas, U., Tõnisson, H., Kont, A. & Pajula, R. 2017. Multidisciplinary approach to studying the formation and development of beach-ridge systems on non-tidal uplifting coasts in Estonia. *Boreal Environment Research*, **22**, 67–81.
- Zanchettin, D., Rubino, A., Traverso, P. & Tomasino, M. 2008. Impact of variations in solar activity on hydrological decadal patterns in northern Italy. *Journal of Geophysical Research*, **113**, D12102.

Tormisusest põhjustatud rannavallide rütmilised mustrid Eesti rannikul

Ülo Suursaar ja Hannes Tõnisson

Meretasemest kõrgemale kerkinud, vahel mattunud, kuid sageli ümbritseval maastikul selgesti eristuvad rannavallide süsteemid on nagu omapärane geoloogiline arhiiv, mis sisaldab teavet mineviku kliima ja veetaseme kõikumiste ning tormide kohta. Mõnikord moodustavad vanad rannamoodustised rütmilisi mustreid, mille teket on soodustanud maakerge ja sette piisav olemasolu. Vähemalt 27 sellist rütmiliste geomorfoloogiliste mustritega piirkonda tuvastati LiDAR-i kõrgusandmete põhjal Eesti jääajajärgselt (geoidi suhtes vertikaalkiirusega 1,7–3,4 mm/a) kerkivatel randadel. Rütmilised rannavallisüsteemid esinevad suhteliselt kiiremini kerkivatel, läände või põhja hästi avatud randadel. Need asuvad peamiselt kõrgusvahemikus 1–21 m, mis vastab vanusele kuni umbes 7500 aastat. Mõnel, kuni 4 km pikkusel profiilil võib loendada umbes 150 üksikvalli. Kümme selgemini väljenduvat, vähem kui 4500 aastat vana rannavallide “mustrit” valiti täpsemaks analüüsiks, et välja selgitada selle nähtuse võimalikke kujunemismehhanisme. Keskmiselt paiknesid vallid üksteisest 19–28 m kaugusel. Arvesse võttes maapinna näiva tõusu kiirust Holotseenis, leiti uuritavate profiilide vanusevahemikud. Detailsemalt käsitletud profiilide puhul esines vallides 23–39-aastane nõrk perioodilisus (üldise keskmisega 31 aastat). Arvestades vallide (ja vanade rannaastangute) suurt korrapärasust, ei saa need peegeldada üksiktorme ega tsunamide, vaid pigem pikaajalisi muutusi tormisuses. Kuigi on võimalik ka panus mingist iseorganiseeruvast sette akumulatsiooni mehhanismist, saab peapõhjusena neid mustreid siduda kvaasiperioodilise 25–40-aastase muutlikkusega, mis on nähtav Eesti pikaajalistes meretaseme vaatlusridades, lainearvutuste ja regionaalsete tormisuse andmetes ning ka NAO indeksis.